Mariner 7 Ultraviolet Spectrometer Experiment: Photometric Function and Roughness of Mars' Polar Cap Surface

KEVIN PANG AND CHARLES W. HORD

Laboratory for Atmospheric and Space Physics, University of Colorado, Boulder, Colorado 80302

The Mariner 7 ultraviolet spectrometer observed the south polar cap of Mars. The near ultraviolet polar spectrum shows the predominance of surface reflection over atmospheric scattering. The intensity of the reflected radiation, I, decreased steeply for a change in solar elevation of only about 10°. Neither a haze layer nor ground inhomogeneity is considered a likely explanation for this observation. An unusual photometric function of the surface is more probable.

An analysis of intensity as a function of the incidence and emission angles (i and ϵ) was made, assuming a photometric function of the form $I \sim \cos^k i \cos^{k-1} \epsilon$ (Minnaert's law) for the surface. Eight model atmospheres, based on information previously known for Mars or from the Mariner 6 and 7 missions, were used to correct for scattering and attenuation effects. The angular inversion revealed a rather high value of about 3 for k. This result is interpreted to mean that the surface reflection is strongly specular as from an icy or glazed surface.

Applying the principle of least variation of the k value with wavelength, it was learned that the atmosphere over the polar region was not as turbid as that over the deserts; and that the ozone, discovered from spectral inversion of the same data, is either low in the atmosphere or trapped in the polar cap.

An hypothesis is advanced to explain the observed phenomena and associated polar features.

I. INTRODUCTION

In 1969 the Mariner 6 and 7 spacecraft flew past Mars while instruments aboard viewed the planet at a resolution and observational geometry never before possible. The ultraviolet spectrometer experiment and some of its results have been reported elsewhere: instrumentation (Pearce *et al.*, 1971), upper atmosphere (Barth *et al.*, 1969, 1971*a*), and topography and polar cap (Barth and Hord, 1971; Hord, 1971). This paper reports results for the photometric function and roughness of the south polar cap surface.

Barth and Hord analyzed ultraviolet spectra of the desert regions of Mars and found the intensity of the reflected radiation to be about three times greater than that scattered from a pure 6.6 mb carbon dioxide atmosphere. It was also learned that the reflectance increases monotonically with decreasing wavelength. They concluded that the ultraviolet reflectivity of the Martian deserts is low and atmospheric scattering predominates over surface reflection in these areas. They attributed the excess scattering to the presence of particulate matter, whose diameters are small compared with the wavelength.

The ultraviolet spectrum of the Mars polar cap is much more intense than that of the desert; a factor of three at 2900 Å and two at 2500 Å. Barth and Hord concluded that the ultraviolet reflectivity of the polar cap is high. A broad absorption feature centered at 2550 Å was observed in the reflectance spectrum, and this was explained in terms of Hartley band absorption by ozone.

If the ozone is in the atmosphere, the amount needed to produce the observed feature was calculated to be 1×10^{-3} cm-atm. Laboratory experiments by Broida

et al. (1970) indicate that ozone may be trapped in solid carbon dioxide.

In addition to the spectral shape or wavelength dependence of the reflectance, the variation of the intensity of the reflected radiation with incidence and emission angles is available for analysis. The reflectance spectrum of the Mars south polar cap differs from its desert counterpart in that light reflected from the surface predominates. The observed contrast is still noticeable down to 2200 Å. Spatial intensity variations observed by the ultra-violet spectrometer correlate well with surface features of the same region in the television pictures. This makes it possible to obtain a photometric function of the polar cap using the angular dependence of the data. Knowing the photometric function, we can deduce some information on the roughness of the polar cap surface.

II. Data

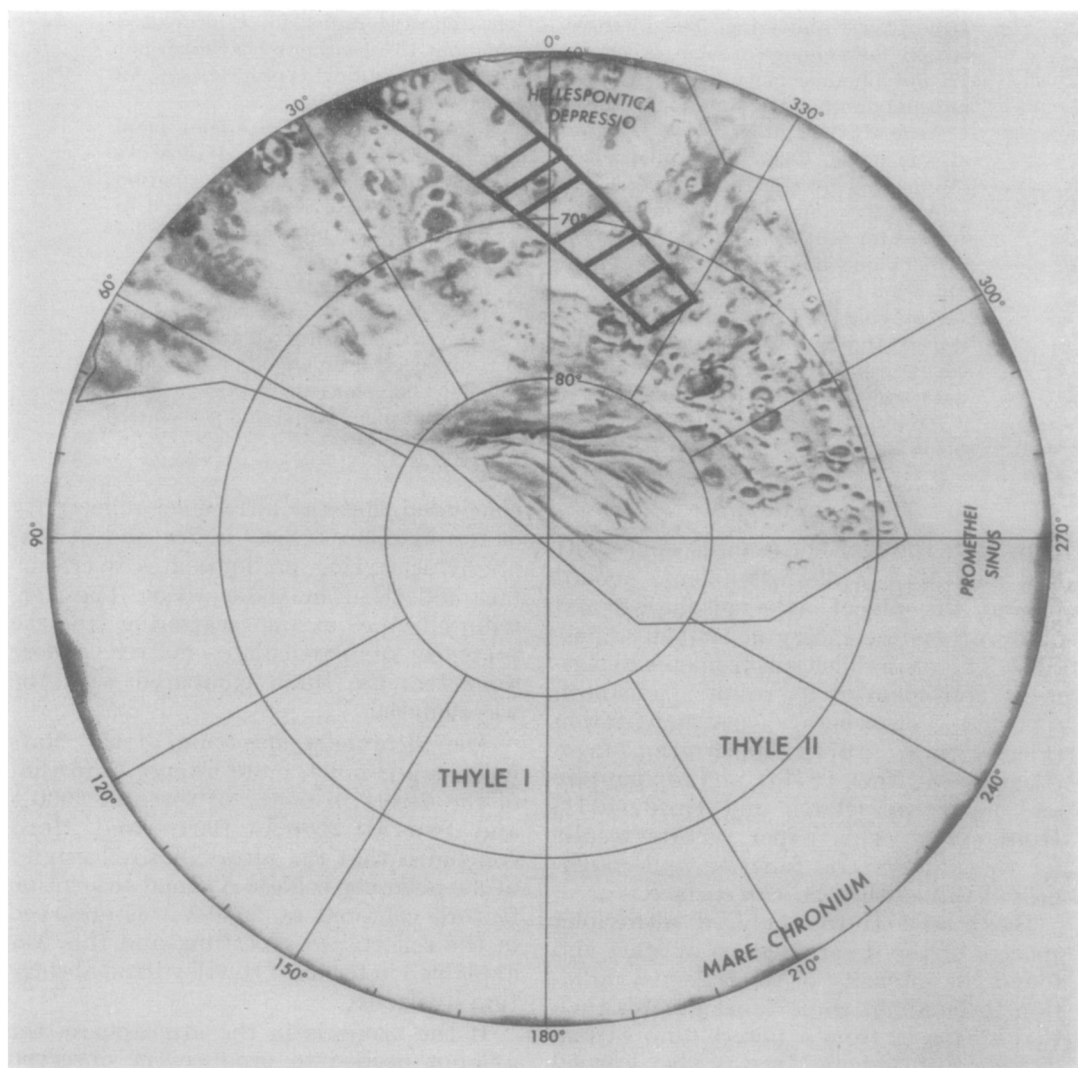The region scanned by the ultraviolet spectrometer is shown on a polar projection

Fig. 1. Map of Mars south polar region. Hatched portion is area observed by Mariner 7 ultraviolet spectrometer.

PHOTOMETRIC FUNCTION OF MARS' POLAR CAP

map of Mars prepared from Mariner 7 television pictures. The area of interest is shown in Fig. 1. The area covered by an individual spectrum varies from about 300×30 km at the top to about 200×20 km at the bottom. Such an area is represented approximately by the length and width of a hatch mark. Hatch marks indicate the locations of the first, 5th, 11th, 20th, 27th, and 33rd spectrum. The latitude and longitude of the area scanned varied from $-66.0°$ to $-74.0°$ and $7.3°$W to $335.4°$W (through $0°$) respectively. The incidence angle ranged from $56.9°$ to $66.5°$, and the emission angle from $41.3°$ to $39.4°$. The Sun's azimuth changed from $5.4°$E to $26.9°$W (through North). The azimuth of observation varied from 53.4W to 75.9W, or $58.8°$W to $49.0°$W from the Sun's azimuth. The phase angle remained constant at $46.3°$ throughout the time of observation.

Thirty-seven contiguous polar cap spectra were studied. Twelve wavelength intervals, centered at 2200, 2240, 2320, 2430, 2500, 2550, 2580, 2655, 2700, 2800, 2850, and 2885 Å, were selected for analysis. Data above 2885 Å were off-scale and thus not available. The data were smoothed by taking averages over three sample numbers (SN) (1 SN ≈ 4.3 Å). Detailed descriptions of the data and their reduction together with averages of individual spectra are given in a separate report (Barth *et al.*, 1971*b*).

How the intensity, observed at a particular wavelength, varies during the course of the polar viewing can be seen in Fig. 2. The open circles represent data points taken at 2800 Å at three-second intervals. The direction of increasing time is from right to left. The quantity plotted along the y-axis is the product of the cosine of the emission angle and the intensity (in units of net solar flux outside the Martian atmosphere, F). The product of the cosine of the emission angle and the cosine of the incidence angle is plotted along the x-axis. Since the emission angle changed very little during the course of observation, the scattergram shows essentially the variation of intensity with the cosine of the incidence angle. The

intensity change is primarily an effect due to decreasing solar elevation, barring the possibilities of ground inhomogeneity.

The magnitude of this intensity change is considerable. The intensity decreases from 0.246 to 0.0979 ($\pi F = 1$). This is a change of about 60%, a rather large decrease for a Sun angle variation of only $9.6°$ at moderate solar elevations. Remarkable darkening at the south polar cap was also seen near both the limb and terminator in far-encounter television pictures (Leighton *et al.*, 1969). It is possible that the phenomenon seen in the ultraviolet and the visible regions of the spectrum have a common cause. The south polar cap shading is most likely an effect due to near grazing angles of observation or a sunset effect, and not due to surface inhomogeneity, since it is seen only near the limb and terminator. Sharp *et al.* (1971) account for this darkening in terms of a haze, while Leovy *et al.* (1971) suggest that it is due to a photometric function of the surface. Unfortunately, the ultraviolet spectrometer scanned only in the vicinity of the terminator and not the limb of the polar cap, and thus we are unable to make a symmetrical comparison.

Possible explanations of the steep intensity change observed in the ultraviolet also include the presence of haze over the polar region and an unusual photometric behavior of the cap itself. We cannot discriminate between these two possibilities on the basis of photometric data alone. However, we have additional information in the form of spectral data.

Let us examine the gross rate of decrease of the uncorrected intensity with the cosine of the incidence angle in different wavelength intervals. This rate is equal to the slope of the straight line of best fit through the data points, determined by standard regression methods. This slope has the values of 2.27, 2.44, 2.20, 2.58, 2.51, 2.74, 2.94, 3.12, 3.12, 2.84, 3.01, and 3.10 for the twelve spectral intervals stated, in order of increasing wavelength. An examination of this set of numbers shows an increase with increasing wavelength. From this, we conclude that if a haze layer is responsible for the intensity
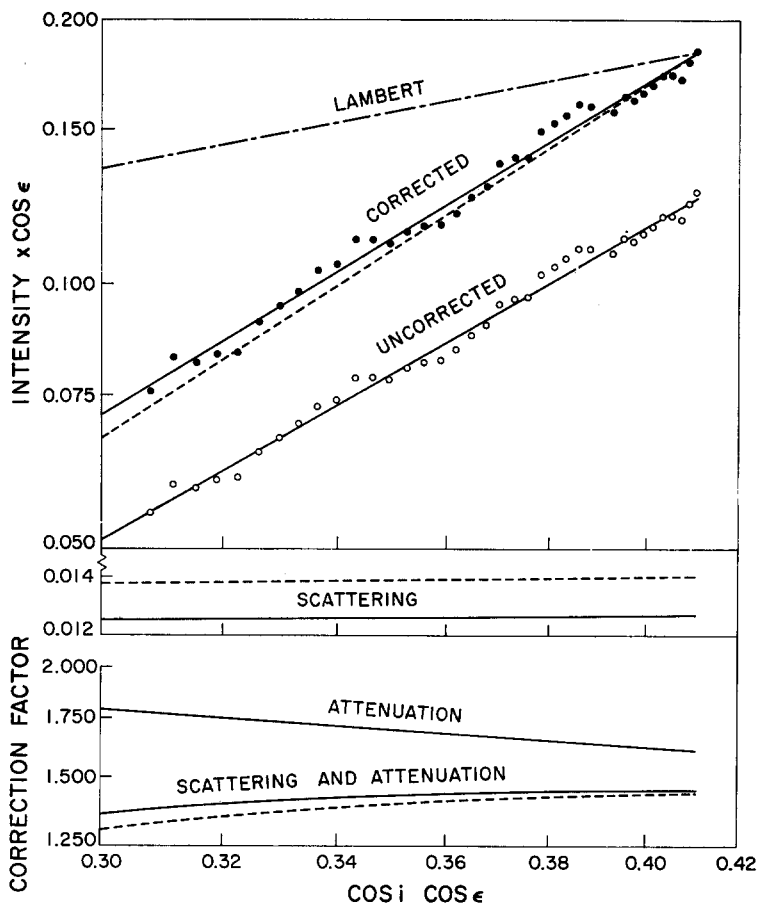
FIG. 2. The upper graph shows the variation of the product of the intensity (at 2800 Å) with os ε vs. cos i cos ε. The lower graph shows the correction factor vs. cos i cos ε.

decrease with increasing optical air mass, then attenuation of the incident and reflected rays alone cannot produce the spectral effect observed. The extinction cross section of particles capable of suspension in the tenuous Martian atmosphere would, in general, be increasing (or at most constant) with decreasing wavelength. This is incompatible with the observations. We will consider the possibility of a haze layer again in the next section taking into account both attenuation and scattering. An alternate explanation of an anomalous photometric function will be derived from an analysis of the data in the next section. We will now consider the problem of surface inhomogeneity.

Two types of surface inhomogeneity can influence the variation of the reflected intensity. These are changes in the degree of ice coverage with latitude and with orientation of topographic slopes. The more completely the condensate covers the ground, the higher the surface albedo should be.

First, the most likely surface albedo variation would be an increase with decreasing latitude, because the thickness of the cap should increase poleward. The effect of such surface inhomogeneity is to decrease the slope of our intensity curve. If this effect exists the true slope would be greater than that found from our analysis.

The surface albedo does not increase indefinitely with snow depth. Extensive airborne observations of albedo of farm

and forest land on Earth show that it increases rapidly with increasing snow depth up to about 13 cm (Kung et al., 1964). Accumulation of snow beyond this limit does not significantly increase the albedo further. The surface albedo may be considered approximately homogeneous once the snow depth passes this point. A limit of 10 cm may be considered as reasonable for the Mars polar region since rocks, gravel and sand (likely constituents of Martian ground) are easier to cover than forest land.

Sharp et al. (1971) observed that the coverage in the Mars polar cap interior (latitude less than $-60.5°$) is essentially continuous. They estimated the cap thickness to be at least tens of meters in the area of the "elephant's footprint" in television picture 7N14. This picture is nested in the area seen in our northernmost spectra (latitude less than $-66°$). From these results it is reasonable to assume that most of the ground cover in this area and south of it attains at least 10 cm thickness. Thus, we will assume that the albedo of the polar cap surface is approximately homogeneous with latitude, when averaged over an area seen in a single spectrum.

If the surface albedo does change with slope orientation it should increase as the azimuth of the slope varies from $0°$ (north-facing) to $180°$ (south-facing), because of increasing ice coverage with less and less solar radiation. In our northernmost spectra the Sun was almost directly north of the area observed, illuminating most strongly the equator-facing slopes. From then on, the azimuth of the sun gradually increased, shining more and more on west-facing slopes. At the same time the azimuth of observation also slowly increased, i.e., the spectrometer saw less and less of north-facing slopes. The effect of this second type of surface inhomogeneity is to decrease the slope of the intensity curve. As before, if this effect exists the true slope would be greater than that found from our analysis.

Sharp et al. (1971) observed ice-free areas and craters with ice only on south-facing inner walls in the outer marginal zone (latitude between $-57°$ and $-58.5°$). Ice-free areas were also observed within the inner marginal zone (between $-58.5°$ and $-60.5°$). However no such features were found in the pole-cap interior. Consequently we will assume that the surface albedo is essentially independent of slope orientation in the area scanned by, and at the resolution of, the uv spectrometer.

To summarize, both types of surface inhomogeneity that are possible for the Mars polar region have the effect of decreasing the slope of the intensity curve. Consequently surface inhomogeneity is an unlikely explanation for the steep intensity decrease observed.

III. PHOTOMETRIC FUNCTION

The intensity of solar radiation at wavelength λ directly reflected from a surface and attenuated by a plane-parallel atmosphere, may be represented by the equation

$$4\pi I_D = 4\pi F \rho_0 f \exp[-\tau(\sec i + \sec \epsilon)], \tag{1}$$

where

πF is the net solar flux outside the Mars atmosphere,

i is the angle of incidence,

ϵ is the angle of emission,

τ is the normal optical thickness,

ρ_0 is the normal albedo of the surface,

f is the photometric function of the surface.

The simplest photometric function that satisfies the reciprocity principle follows from Minnaert's law,

$$f = \cos^k i \cos^{k-1} \epsilon. \tag{2}$$

k is a constant indicative of the surface roughness and is sometimes called the "smoothness factor" (Sytinskaya, 1949). For a Lambert surface $k = 1$ and Minnaert's law reduces to Lambert's law, i.e., $f = \cos i$. For a very smooth surface $k \gg 1$. k may depend on the azimuth of observation A, or in the case of planetary photometry, the phase angle α. For example, $k = 0.5$ for the full Moon but is nearly equal to 1 for phase angles greater than $90°$.

Our goal is to determine k for the Mars polar cap, and deduce the roughness of the

cap surface. The intensity observed by the spectrometer I_{obs} consists of not only the directly reflected and attenuated component I_D, but also a component diffusely reflected from the atmosphere I_d. In practice it is impossible to separate the two components. However, we can make a theoretical correction for the diffuse component by assuming a model atmosphere. We will discuss this point fully later. Equation (1) can be written with the intensity in units of πF,

$$4\pi(I_{obs} - I_d)/4\pi F$$
$$= \rho_0 \cos^k i \cos^{k-1} \epsilon$$
$$\times \exp[-\tau(\sec i + \sec \epsilon)]. \quad (3)$$

For an optically thin atmosphere, the logarithmic form of this equation can be inverted if F, i, ϵ, and either ρ_0 and k (surface parameters) or I_d and τ (atmospheric parameters) are known. In the first case

$$\ln[4\pi(I_{obs} - I_d)/4\pi F \cos^k i \cos^{k-1} \epsilon]$$
$$= \ln(\rho_0) - \tau(\sec i + \sec \epsilon). \quad (4)$$

This is an equation of a straight line

$$Y = a + bX. \quad (5)$$

Statistical evaluation of variations of $\ln[4\pi(I_{obs} - I_d)/4\pi F \cos^k i \cos^{k-1} \epsilon]$ with $(\sec i + \sec \epsilon)$ can yield estimates of the slope τ and the intercept $\ln(\rho_0)$. I_d, the correction term, can be determined by successive iteration and the correct choice of I_d should yield the known value of ρ_0.

In the second case

$$\ln[4\pi(I_{obs} - I_d)\cos\epsilon/4\pi F] + \tau(\sec i + \sec \epsilon)$$
$$= \ln(\rho_0) + k\ln(\cos i \cos \epsilon). \quad (6)$$

Again, regression analysis of the variation of the left-hand-side values with $\ln(\cos i \cos \epsilon)$ can give estimates of the slope k and the intercept $\ln(\rho_0)$.

The above analysis was made without taking into consideration that k may vary with the azimuth or phase angle, as in the case of the Moon. To overcome this difficulty we may perform our analysis in a small range of A or α, and assume as a first approximation that k does not change much within this range. As a second approximation, we assume that the area

scanned by the spectrometer was covered by horizontal surfaces which follow the same photometric function.

Equation (6) was used in an angular inversion of the polar cap data. The correction terms for diffuse reflection, I_d, and attenuation, $\tau(\sec i + \sec \epsilon)$, were computed for eight model atmospheres:

1. 6.6 mb pure CO_2 atmosphere.
2. Desert atmosphere with "violet" haze. Its optical thickness is approximately three times that of Model 1 but due entirely to Rayleigh scatterers. The values used are averages found by Barth and Hord (1971) from spectral inversion of the ultraviolet data taken over the Mars desert regions.
3. 6.6 mb CO_2 atmosphere on top of O_3 layer. Values for ozone were derived by Barth and Hord by spectral inversion of ultraviolet data taken over the polar region.
4. Desert atmosphere on top of O_3 layer.
5. 6.6 mb CO_2 uniformly mixed with O_3.
6. Desert atmosphere uniformly mixed with O_3.
7. O_3 layer on top of 6.6 mb CO_2 atmosphere.
8. O_3 layer on top of desert atmosphere.

For Models 1 and 2, I_d was calculated from the single scattering formula with the Rayleigh phase function,

$$4\pi I_d/4\pi F$$
$$= (3/16)\,\varpi_0 \cos i(1 + \cos^2 \Theta)$$
$$\times \{1 - \exp[-\tau(\sec i + \sec \epsilon)]\}/$$
$$(\cos i + \cos \epsilon). \quad (7)$$

Multiple scattering and illumination of the atmosphere by the ground (and vice versa) are neglected since the Martian atmosphere is optically thin even in the near ultraviolet. In the first two models, ϖ_0, the albedo of single scattering, is 1, and $\tau = \tau_R$, the Rayleigh optical thickness. The scattering angle, Θ, is 133.7° for all spectral intervals and models. For Models 3 and 4, the same formula and values are used to compute I_d. However $\tau = \tau_R + \tau_{O_3}$ in the correction term for the attenuation. For Models 5 and 6, Eq. (7) is again used, but with $\varpi_0 = \tau_R/\tau$ and $\tau = \tau_R + \tau_{O_3}$. The same value of τ was used in calculating the correction for the attenuation. For Models 7 and 8, Eq. (7)

is modified to include an extra attenuation factor, $\exp[-\tau_{O_3}(\sec i + \sec \epsilon)]$. In Eq. (7) $\tau = \tau_R$, but is equal to $\tau_R + \tau_{O_3}$ in the attenuation term in Eq. (6).

The photometric function of a surface is determined primarily by its irregularities. The wavelength of light is much less than the size of these irregularities for most natural surfaces. Consequently, the value of k ideally should not vary with λ provided that the surface absorption does not change with λ. This assumption is made for the Mars polar cap since laboratory measurements show that the reflectance of freshly precipitated solid carbon dioxide (the most likely polar cap constituent) is large and constant with wavelength between 2000 Å and 3000 Å. Consequently, the model atmosphere that leads to the least variation in the k value with λ will be considered to fit our data best.

Simple linear regression methods were used to analyze the data. A FORTRAN program reads uncalibrated data numbers, corrects for the background, and converts the results into units of πF, after taking into account the instrumental sensitivity. The diffuse reflection and attenuation is corrected. The program then calculates the logarithm of the intensity, corrected for atmospheric effects, left-hand side of Eq. (6), and plots it against $\ln(\cos i \cos \epsilon)$ in a scattergram; finds the equation of best fit by the method of least squares, and computes the correlation coefficient and standard deviations. An example of such an analysis is Fig. 2. The procedure involves subtracting the diffusely reflected radiation (curves marked "SCATTER-ING") from the observations (open circles labeled "UNCORRECTED") and then multiplying by the correction factor (curve marked "ATTENUATION") to arrive at the intensity corrected for atmospheric effects (black circles labeled "COR-RECTED"). The net effect is illustrated as a total correction factor (curves marked "SCATTERING AND ATTENU-ATION"). The model used in this particular example is Model No. 3 in which $\tau_R = 0.05$ at 2800 Å. The broken lines denote computational results using values interpolated from tables published by Coulson et al. (1960) with all orders of scattering taken into account. Since the Martian atmosphere is optically thin, the final results of this more involved procedure differ from those of our simpler single scattering method (solid lines) by only a few percent. The slope of the regression equation is k, the "smoothness factor" desired. Values of k are given as functions

TABLE I

VARIATION OF k WITH WAVELENGTH AND MODEL NUMBER

λ (Å)	Model No.							
	1	2	3	4	5	6	7	8
2200	2.52	2.78	2.42	2.68	2.36	2.53	2.30	2.31
2240	2.75	3.17	2.60	3.02	2.52	2.77	2.43	2.46
2320	2.53	3.18	2.24	2.89	2.08	2.37	1.95	1.88
2430	3.05	4.22	2.53	3.70	2.26	2.66	2.07	1.94
2500	3.12	4.82	2.48	4.63	2.11	2.69	1.88	1.80
2550	3.36	4.93	2.69	4.80	2.32	2.90	2.09	2.03
2580	3.65	6.36	3.02	5.70	2.61	3.40	2.35	2.39
2655	3.72	5.53	3.17	4.99	2.87	3.60	2.66	2.78
2700	3.68	5.34	3.23	4.89	2.99	3.75	2.81	3.03
2800	3.23	4.26	3.01	4.03	2.90	3.59	2.81	3.21
2850	3.38	4.30	3.24	4.17	3.18	3.91	3.12	3.67
2885	3.43	4.24	3.36	4.14	3.30	3.99	3.26	3.82
Mean	3.20	4.43	2.83	4.15	2.63	3.19	2.48	2.62
Standard deviation	0.42	1.05	0.38	0.93	0.41	0.58	0.45	0.69

of the wavelength and model number in Table I.

IV. SURFACE ROUGHNESS

An examination of Table I shows that the values of k are rather high regardless of which model is used to correct for the atmospheric effects. These large slope values are consistent with the large decrease in the observed intensity for a change in solar elevation of about $10°$. Such a steep intensity variation is not compatible with reflection from a Lambert surface ($k = 1$, top curve in Fig. 2), unless the effect is attributed to a haze overlying the surface. Computations show that a haze layer of greater optical thickness than that used in the models is required to produce the observed effect. However, this leads to other difficulties.

The standard deviations of the k values in Table I show that a 6.6mb pure CO_2 atmosphere with a layer of ozone near the ground gives the least spread in the k values. The same atmosphere with the ozone either not in it, or uniformly mixed with the major constituent, is a close second choice. A hazy desert atmosphere does not fit the data well. An optically thicker atmosphere would produce a still greater spread in the k values and thus is unacceptable. This shows that a haze layer is probably not the cause of the large intensity decrease observed. On the basis of this analysis, it seems that the atmosphere over the polar region scanned is not as turbid as that of the deserts. Ozone, discovered from the wavelength dependence of the reflectance, is more likely to exist low in the atmosphere or may be trapped in the polar cap, in order to be consistent with the spectral data.

Comparison with laboratory reflection measurements yields very interesting results. Sytinskaya (1949) measured the photometric function of many different surfaces under the special opposition-like condition, i.e., observing close to the direction of incidence. For this special case of $i \approx \epsilon$,

$$f = \cos^k i \cos^{k-1} i = \cos^{2k-1} i = \cos^q i,$$

(8)

where

$$q = 2k - 1, \quad \text{or} \quad k = \tfrac{1}{2}(q + 1). \quad (9)$$

Numerous laboratory and field measurements support this formula for the great majority of natural surfaces within experimental error. The q values Sytinskaya found and their k equivalents (in parentheses) are summarized as follows:

$q > 1 (k > 1)$ for polished surfaces

$q = 1 (k = 1)$ for an ideal orthotropic surface following Lambert's law

$q = 0.85–0.92$ for photometric screens $(k = 0.93–0.96)$

$q < 1 (k < 1)$ for most natural objects: rocks, 0.1–0.6 (0.55–0.8); sand, 0.3–0.5 (0.65–0.75); gravel and pitted surfaces, 0.1–0.2 (0.55–0.6); vegetation, sometimes down to −0.14 (0.43), never above 0.4 (0.7)

Although the observational geometry for the Mariner 7 polar scan is not exactly the same as these laboratory experiments, it is not very different. The angle between the incident and reflected rays is only about $45°$. Thus, we can still make the analogy that the Mars polar region scanned resembles a polished surface more than any of the other objects mentioned above.

An order-of-magnitude estimate may be made on the size of the irregularities on the polar cap surface. This should not be confused with the topographical features, which show up as bright ridges or dark valleys. It is the microrelief of the surface that determines the general slope of the intensity curve, and thus the photometric function (see Fig. 2). Observations by Barabashov and Chekirda (1960) showed that dustlike substances with grain size of 0.06mm diameter yield a pattern of reflection which closely obeys Lambert's law. Using this result as an upper limit, we deduce that the dimensions of the irregularities are less than 60μ. The strongly specular nature of the surface reflection leads us to infer that the polar

region scanned is predominantly covered with icy or glazed material.

As stated in Section II, the slope of the intensity curve, k, would be higher if there were no surface inhomogeneity. So the effects of such inhomogeneity, if present, reinforce, not weaken, the above conclusion.

V. DISCUSSION

An icy or glazed surface is the most likely explanation for the steep intensity variation found for the small change in observational geometry. The formation of such a surface under Martian conditions seem to be a difficult phenomenon to explain based on our experience of similar processes with water on Earth. Because of the extremely low temperature and pressure of the Martian polar regions, any mechanism involving a transition through the liquid phase is out of the question, since solid carbon dioxide and water (a possible minor constituent) do not liquify under such conditions. Thus a nonaqueous scheme is necessary. Recent laboratory experiments with solid carbon dioxide suggest a solution.

Experiments done at the Laboratory for Atmospheric and Space Physics by Kelly (1971) showed that, in a pure CO_2 atmosphere at a pressure of about 10 mm Hg, the gas consistently condensed as clear ice on a low temperature surface. This carbon dioxide ice looks very much like ordinary water ice. Introduction of a non-condensing buffer gas, such as nitrogen, into the system is essential for the formation of carbon dioxide frost. Broida (1970) observed a glassy material forming out of a mixture of gaseous CO_2 and ozone maintained at approximately Martian polar temperatures.

From the Mariner 6 and 7 and the laboratory results, we hypothesize that the following processes take place in the polar regions of Mars and that they are responsible for some of the polar phenomena observed:

1. The atmosphere of Mars is nearly pure carbon dioxide.

2. When the ground temperature drops to 148°K during local autumn, gaseous carbon dioxide condenses directly from the atmosphere onto the ground and forms ice layers.

3. At about the same time clouds appear in the atmosphere through the condensation of CO_2 on ice nuclei in the gas. These clouds may constitute the polar hood.

4. Precipitation of solid CO_2 from the atmosphere-"snow"-together with the direct deposition mentioned in 2 continuously build up a polar cap in late autumn and winter. The precipitation continues until the lower atmosphere is no longer cold enough and/or the ice nuclei are depleted.

5. Even after the precipitation has stopped, the ground is still at the freezing point of CO_2 as long as it has a snow cover. The gaseous CO_2 continues to condense on this cold surface as clear ice. This process is responsible for the icy or glazed appearance of the cap surface discovered by the Mariner 7 ultraviolet spectrometer. Since this process fuses fine fluffy snow crystals into "glazed" surfaces of large textural scale, the quasi-specular reflection from such surfaces may explain why the observed bidirectional reflectance of the Mars polar cap is lower than that of laboratory samples of CO_2 and H_2O frosts (Kieffer, 1970).

6. In the early spring the clouds dissipate, exposing the cap surface to solar heating. This results in the sublimation of the glazed snow. The disappearance of the snow uncovers the ice layers which were formed in the last autumn. Reflection from a clear-ice-coated mineral surface is strongly specular. The radiant energy is now reflected in the forward direction at the expense of other direction. Consequently such a surface would look darker than the original diffusely reflecting mineral surface when viewed from the Earth (near-backward directions). These darkened mineral surfaces constitute the so-called polar collar. Photometric observations of the polar collar show that is it darker than other surfaces on the planetary disk (Capen, 1971). This suggestion is also consistent with polarimetric and colorimetric observations indicating

that the polar collar has a smooth surface.

7. The ice layers are the last to sublime. After the bright polar cap has receded from an area the dark polar collar follows, and in so doing, returns the mineral surface to its original summer appearance.

8. Decalibrated television pictures show no suggestion of a polar collar at the time of the Mariner 7 flyby. At the same time Earth-based telescopes observed either a very faint collar or none at all. If the atmosphere drops to freezing before the ground does, snow would fall before ice layers can be formed; thus no polar collar will be observed the following spring and summer. When the recession rate of the cap is at a minimum this hypothesis predicts that no collar should be seen. No new ice layers are exposed and previously exposed layers can "catch up" with the snow cap. At the maximum recession rate the collar should be widest and most prominent. The above predictions agree with ground observations and may explain why no collar was seen by the Mariner 7 television camera.

The above hypothesis makes no use of transitions through the liquid phase and does not involve water, and therefore avoids the difficulties encountered by the aqueous hypotheses, e.g., the low temperature and scarcity of water. Furthermore, it agrees qualitatively with photometric, colorimetric, polarimetric, and recession data. A detailed exposition of the above outline will be presented in a future report. Extensive observations by the Mariner '71 missions and more laboratory measurements should lead to a better understanding of these processes.

Since reflection from a moist level surface is also strongly specular, this method may be a good way of identifying moist areas over the desert regions in future missions to Mars.

ACKNOWLEDGMENT

REFERENCES

BARABASHOV, N. P., AND CHEKIRDA, A. T. (1960). A study of the rocks most closely resembling the surface constituents of the Moon. *Soviet Astron.-AJ* **3**, 827–831.

BARTH, C. A., FASTIE, W. G., HORD, C. W., PEARCE, J. B., KELLY, K. K., STEWART, A. I., THOMAS, G. E., ANDERSON, G. P., AND RAPER, O. F. (1969). Mariner 6: Ultraviolet spectrum of Mars upper atmosphere. *Science* **165**, 1004–1005.

BARTH, C. A., AND HORD, C. W. (1971). Mariner 6 and 7 ultraviolet spectrometer results: Topography and polar cap. *Science* **171**, 197–201.

BARTH, C. A., HORD, C. W., PEARCE, J. B., KELLY, K. K., ANDERSON, G. P., AND STEWART, A. I. (1971a). Mariner 6 and 7 ultraviolet spectrometer experiment: Upper atmosphere data. *J. Geophys. Res.* **76**, 2213–2227.

BARTH, C. A., HORD, C. W., PEARCE, J. B., AND KELLY, K. K. (1971b). Mariner 6 and 7 ultraviolet spectrometer experiment: Lower atmosphere and surface data. *Icarus*, to be submitted.

BROIDA, H. P. (1970). Personal communication.

BROIDA, H. P., LUNDELL, O. R., SCHIFF, H. I., AND KETCHESON, R. D. (1970). Is ozone trapped in the solid carbon dioxide polar cap of Mars? *Science* **170**, 1402.

CAPEN, C. F. (1971). Personal communication.

COULSON, K. L., DAVE, J. V., AND SEKERA, Z. (1960). "Tables Related to Radiation Emerging from a Planetary Atmosphere with Rayleigh Scattering." University of California Press, Berkeley and Los Angeles.

HORD, C. W. (1971). Mariner 6 and 7 ultraviolet spectrometer experiment: Photometry and topography of Mars. *Icarus*, to be submitted.

KELLY, K. K. (1971). Personal communication.

KIEFFER, H. (1970). Interpretation of the Martian polar cap spectra. *J. Geophys. Res.* **75**, 510–514.

KUNG, E. C., BRYSON, R. A., AND LENSCHOW, D. H. (1964). Study of a continental surface albedo on the basis of flight measurements and structure of the Earth's surface cover over North America. *Monthly Weather Rev.* **92**, 543–564.

LEIGHTON, R. B., HOROWITZ, N. H., MURRAY, B. C., SHARP, R. P., HERRIMAN, A. H., YOUNG, A. T., SMITH, B. A., DAVIES, M. E., AND LEOVY, C. B. (1969). Mariner 6 and 7 television pictures: Preliminary analysis. *Science* **166**, 49–67.

LEOVY, C. B., SMITH, B. A., YOUNG, A. T., AND LEIGHTON, R. B. (1971). Mariner Mars 1969:

Atmospheric results. *J. Geophys. Res.* **76**, 297–312.

PEARCE, J. B., GAUSE, K. A., MACKEY, E. F., KELLY, K. K., FASTIE, W. G., AND BARTH, C. A. (1971). The Mariner 6 and 7 ultraviolet spectrometers. *Appl. Opt.* **10**, 805–812.

SHARP, R. P., MURRAY, B. C., LEIGHTON, R. B.,

SODERBLOM, L. A., AND CUTTS, J. A. (1971). The surface of Mars, 4, south polar cap. *J. Geophys. Res.* **76**, 357–368.

SYTINSKAYA, N. N. (1949). Determination of a degree of smoothness of the surfaces of planets by photometric methods. *Uch. Zap. Univ. Leningrad.* (No. 116), 123–137.